Steer Guidance Of Autonomous Agricultural Robot Based On Pure Pursuit Algorithm And LiDAR Based Vector Field Histogram

Rai Bijay[1*], Matsa Amarendra[2], and Datta Asim[3]

[1] Department of Electrical and Electronics Engineering, Sikkim Manipal Institute of Technology, Rangpo, Sikkim- 737136, India
[2] Department of Electrical Engineering, Mizoram University, Mizoram, Aizawl- 796004, India
[3] Department of Electrical Engineering, India, Tezpur University, Tezpur, Assam-784028, India
[*] Corresponding author. E-mail: bijay.r@smit.smu.edu.in

Received: Mar. 24, 2022; Accepted: Nov 05, 2022

The application of autonomous robots has been increasing in agriculture sector to substitute human labour and to improve the production yields. A self-sufficient robot is intended to accomplish specific jobs in different locations of the working field area, thereby an economical and effective navigation system for differential wheeled mobile robots is a paramount importance. In this paper, an autonomous navigation system of an agricultural mobile robot is proposed using pure pursuit algorithm (PPA) which is also assisted by vector field histogram (VFH). PPA autonomously guides towards waypoints, whereas the VFH algorithm helps the vehicle steer away for obstacles. The 2-dimensional light detection and ranging (LiDAR) sensors are used to monitor through the VFH algorithm. Minimum number of waypoints are set in PPA for convenience on map setup. Several indicators such as distance covered by robot, number of iterations required for completion of travel, etc., are investigated with the variable settings in PPA algorithm. Result analysis shows that mobile robot can travel at speed range of 2.5-25 km/hr with obstacle evasion which is adequate for agricultural mobile robots.

Keywords: agricultural autonomous robot, vector field histogram (VFH), pure pursuit 33 algorithm, light detection and ranging (LiDAR), obstacle avoidance

http://dx.doi.org/10.6180/jase.202310_26(10).0002

1. Introduction

Despite being an agricultural superpower, India lacks efficient agricultural water management. Rain provides 62 percent of the water, while irrigated supplies provide 37 percent [1]. In rural places, the majority of water (about 85 percent) is generally wasted. Younger generations are gravitating toward urban-type jobs, away from agriculture, resulting in labour shortages for farmers. As a result, autonomous navigation robots will play an essential role in agriculture, filling the hole and increasing output yields. Agriculture always necessitates a large amount of water and chemicals. The traditional method of agriculture wastes a lot of these resources. Precise farming procedures help you save money by reducing resource consumption. The use of autonomous robots for irrigation and pesticide and fertiliser application can help farmers be more precise [2].

Easy procedures, such as the application of pesticides and irrigation, need simple navigation. India's tough environment has exacerbated the difficulties of agricultural labour; exceptional midday heat waves make it challenging for farmers to work in the field. Automated machines can play a crucial role in such operational areas. A recent government survey suggested that 32 percent of the rural population of India is illiterate, compared to 15 percent of the urban population [3]. India is a delicate market where technological acceptance is not dependent just on performance, but also on simplicity of makeup, affordability, and

sustainability. Farmers embrace technology in a steady, stepwise learning manner. Advanced technologies based on machine learning and data science will be unacceptably expensive and unpredictable to operate for farmers. There is no consensus adopted by any country about the best practices to use automated agriculture robots, confusion still arises on whether to make a robot completely human free or it should need remote monitoring and control [4, 5]. Advanced autonomous robots are reliant on IoT systems [6] designed for internet connectivity in rural areas has a limited bandwidth that is unsuitable for high-speed applications. The VFH and PPA hybrid systems based on a geometrical algorithm while using contemporary LIDAR sensors must be adequate technology to Indian farmers.

Different designs of agricultural robots have been designed primarily for SAE level-2 and level-3 [2] autonomy, which require the least amount of human attention in the field. The mobile robot's performance depends on its ability to recognise and avoid obstacles. Intelligent techniques such as fuzzy logic control technique [7], neural network technique [8], and others have been used to implement certain heuristic methods for detecting impediments and controlling direction. Due to inexact outcomes, fuzzy logic control systems are not always appropriate. Regular rule updates are required to improve accuracy, as well as extensive testing and validation. For a satisfactory and optimal output, the neural network method necessitates a huge amount of data and training. Controlling heuristic algorithms also necessitates the use of a professional operator [9]. For an indoor condition for a mobile robot, a solo-camera vision and ultrasonic sensor-based navigation system is provided [10]. Some agricultural robots use computer vision in conjunction with other sensors to improve GPS data for autonomous navigation, but such approaches are susceptible to ambient lighting, which is a major drawback in an outside context [11]. A gaze-controlled architecture has a fuzzy-integrated and condition-clarified preference for robot navigation, allowing the fuzzy degree sets to be dynamically enabled when the neighbouring state changes [12]. GPS sensor data can be used with motion sensor data to correct high- and low-frequency defects caused by bias and multi-path errors [13]. The strength of a robot's control and monitoring algorithm determines its speed and accuracy. The control and monitoring algorithm must be dependable in order to work in a variety of circumstances and challenges. The main features of navigation include localization, perception, motion control, and cognition [12, 14]. Localization, mapping, path planning, and other aspects of autonomous navigation algorithm development must be considered. Wheeled mobile robots (WMRs), for example, are commonly utilised and rely solely on the wheel drive mechanism for navigation [15]. In robot navigation, deep reinforcement learning (DRL) is utilised since it requires a huge amount of sensor data and a lengthy training period [16]. Bosch Deepfield robotics created the Bonirob robot to eradicate weeds at a rate of 10 Hz. The robot was created utilising vision-based deep learning methodology [17]. Simultaneous localization and mapping (SLAM) is a technique for creating a map in an unknown place, then customising a localization algorithm to regulate the robot's current condition and approaching the objective using a path scheduling module [18]. If precision and accuracy are more important than cost in a large-scale field situation, the Mesh-SLAM technique can help. The internet of things concept can improve scalability and flexibility by making the system modularized such that additional functioning sensor modules can be easily added/modified [19]. To avoid collisions in the projected trajectory, a quadrupole potential field (QPF) approach is proposed [20]. Autonomous robots require dependable sensors and actuators that are appropriate for the working environment. The modern laser-based LiDAR sensor is a reliable sensor found in the majority of advanced autonomous cars. Because global positioning cannot be assured in the sphere of operations indefinitely, three complementary technologies have been developed. Modern perception-based navigation can make use of LiDAR, vision, and ultrasonics. It gives agricultural robots operating for autonomous navigation a consistent intelligent behaviour [21]. Scanning is available for 2-dimensional and 3-dimensional obstacle augmentation. One of the first steps toward prototype development and commercialization is agricultural robot simulation. LIDAR sensors based on lasers are more precise today. They provide quick and accurate scanning for 2-dimensional and 3-dimensional obstacle augmentation. In many situations, modern autonomous passenger vehicles use artificial intelligence, but this comes with the duty of gathering adequate and high-quality data [22]. The study discusses the modelling and simulation of a farm robot that uses the PPA algorithm for navigation. The VFH algorithm is used to assist the system in steering guidance. The area is scanned using a 2D 360-degree LiDAR sensor. PPA is a simple algorithm that follows the predetermined waypoint coordinates until the last point is reached. PPA The algorithm may be run on a 16/32-bit microcontroller, making it suitable for use in a small autonomous robot system. PPA waypoints were specified as different goal coordinate (x,y) sites in the real world, comparable to GPS position coordinates. The VFH algorithm is a quick method that helps robots steer away from obstacles using LiDAR sensors. It can be imple-

mented in an 8/16 bit microcontroller-based device. For the infrequent appearance of smaller obstacles ahead of the robot, the performance was satisfactory.The methodology can be applied to prototypes of electric vehicles with low energy consumption and small-scale compute devices. The mapping strategy for the navigation system is based on 2D LIDAR sensors.

2. Pure pursuit algorithm

For its classic simplicity of operation, the pure pursuit algorithm (PPA) is a common guiding controller algorithm widely utilised in mobile robotics and autonomous vehicle control. PPA instructs the vehicle to follow a list of waypoints in a specific order until all of them are covered. In terms of divergence from the reference trajectory, the robot's speed and the look-ahead distance of path points are key factors. The curvature dimensions are computed using the pure-pursuit approach to take the vehicle from its current position to its final position. The PPA controller may be harmed if the look-ahead distance value is incorrectly chosen. The algorithm's earlier shortcomings have been overcome by recent breakthroughs in dynamical adjustment of the lookahead parameters. However, such an algorithm necessitates a large number of sensors, more data, and computing in order to comprehend the environment. The controller overshoots for shorter look-ahead distances and higher velocity, generating oscillation in the movement trajectory. Sharp turns in the trajectory cannot be followed accurately at higher look-ahead distances due to the controller's large curvature radius. The robot proposed in the research has been tested in a specific scenario with several PPA parameter values. The smallest number of waypoints reduces oscillations, ensures robot movement stability, and provides operator convenience. There have been numerous advanced PPA systems developed [3, 5]. Using GPS data, a fuzzy controller-based PPA accomplished autonomous driving at speeds above 70 km/h [3]. To address the delay of steering actuators, a curve fitting PPA steering technology [5] can be implemented. Although using a mathematical approach to replace the kinematic model with a dynamic model can be an accurate way to manage robots, some studies [23] suggest that the kinematic model performs rather well for slow speed pure chase robots. The merger of PPA and the Kuhn-Munkres (KM) optimal matching algorithm yields an optimal guidance method for unmanned aerial vehicle interception of moving targets [24]. The PPA and a curvature velocity approach have been used to achieve local navigation for electric vehicles. The system is capable of dealing with complex manoeuvres and overcoming the problem of local minima [25].

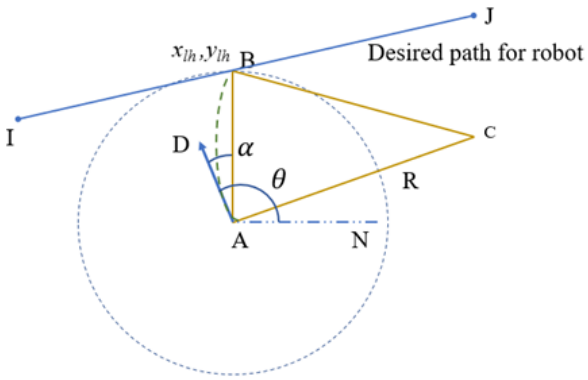

Fig. 1. Conceptual representation of PPA.

The PPA algorithm is conceptually depicted in Fig. 1. The lookahead distance between the robot's position (x,y) and the point of path intersection is lAB (x_{lh},y_{lh}). The LBJ line segment represents the path that the robot should go. Initially, the car is pointed towards the direction of AD. The radius of curvature R is used to create the arc AB with the centre point C. The angle DAB between the vehicle and the radial line lAB is. The angle represents the vehicle's orientation with relation to the x-axis. Eq. (1) is derived [11] using geometrical methods as follows:

$$R = l_{AB}/(2\sin\alpha) \tag{1}$$

where

$$\alpha = \theta - \arctan((y_{lh} - y)/(x_{lh} - x)) \tag{2}$$

Eq. (2) is for the angle α between lookahead direction and orientation f robot. Considering length of the robot is L, the steeting angle γ is given as,

$$\gamma = \arctan(\frac{L}{R}) \tag{3}$$

The steering angle γ is required by the mobile robot to move towards the lookahead points. Based on the concept, PPA is developed to create lookahead points on line interconnecting waypoints, then chase theh lookahead poinsts until end waypoints is reached.

3. Vector field histogram (VFH)

The vector field histogram (VFH) is a fast computable two-stage data-reduction process in taking data from a radial sensor. The data represent the surrounding space and obstacles in 2D space.

Methods for obstacle identification using machine vision have been the focus of several image sensor experiments. Common techniques include background subtrac-

tion and frame subtraction [26]. Kulchandani and Dangarwala [27] has examined a number of techniques for detecting moving objects with a single fixed camera. The background and frame subtraction approaches cannot produce accurate detection results when the backdrop is complicated or has changed, i.e. when the agricultural equipment is in motion. Using machine learning algorithms to detect barriers requires prior knowledge of the obstacles, such as their shape and texture, which is typically not attainable with simple machines [28].

VFH converts Cartesian coordinate map to a polar density map for simpler representation. Borenstein and Koren [29] developed the virtual force field (VFF) method based on potential field method. The paper focuses on the design of PPA based mobile robot assisted by VFH algorithm to prevent collision on obstacles [30]. Dynamic vector based repulsive field algorithm can be used to improve decision making for obstacle avoidance [31]. The VFH algorithm carries out the detection of obstacles and guides the mobile robot towards open ways to the target waypoint. The VFH world model is updated continuously for scanned data from LiDAR sensors. Using the sensor data from grid coordinates of current location, a polar histogram of all direction is obtained. Sectors of the radial polar histogram is created to divide the scanned areas into different zones. Next the algorithm chooses the most suitable sector with low polar obstacle density then provides steering angle for robot to move in the direction [32]. VFH algorithm uses force field to create a repulsive force vector by objects. The vector force magnitude $m_{(m,n)}$ by a grid coordinate (m, n) is proportional to the certainty value $c_{(m,n)}$ and inversely proportional to the distance $d_{(m,n)}$ between the object and robot, as represented by Eq. (5). Certainty values represent the conformity of obstacles, $d_{(m,n)}$ is the distance from the robot to grid coordinate (m, n).

$$\beta_{m,n} = \tan^{-1} \frac{(y_n - y_0)}{(x_m - x_0)} \tag{4}$$

$\beta_{m,n}$ is the orientation of obstacle, where the total angle steps $n = 360/A_a$ any discrete angle $\rho = k$. A_a is the resolution angle, $k = 0, 1, \ldots, n-2, n-1$, sector k is given as $k = integer(\beta_{m,n}/\alpha)$. h_k is the histogram polar obstacle density bearing the summation of all grid coordinate forces in a particular sector k as expressed by Eq. (5). The steering is guided towards the direction with least h_k

$$F_{(m,n)} = (c_{m,n})(a - bd_{m,n}) \tag{5}$$

$$h_k = \sum_{m,n} F_{m,k} \tag{6}$$

Constants a and b are chosen such that force $F_{m,n}$ becomes zero for furthermost obstacle detectable by the sensor. h_k is the very noisy in nature, to filter the value averaging of $2T$ terms is performed, where T is decided by the user.

$$h_{fk} = \frac{h_{k-T} + 2h_{k-T+1} + \cdots + Th_k + 2h_{k+T-1} + h_{k+T}}{2T+1} \tag{7}$$

where h_{fk} is the filtered value of h_k and T is the number of terms used for filtering. The sector with the least value and near to target direction is chosen as right direction for propagation of mobile robot.

4. LiDAR technology

A typical LiDAR uses laser beams to scan a given field of view (FoV). A rapid optical transmitter-receiver device uses a modulated near infrared beam to identify objects in the environment. To rotate and fast scan a vast region, a mechanical or solid-state beam steering mechanism is used. LiDAR technology is resistant to the effects of ambient lighting, making it suitable for agricultural use. Furthermore, the seeing range is greater than that of vision cameras. The lower cost of LiDAR devices in recent years has sparked interest in their use [33]. A study published in [34] used a 3D LiDAR-based navigation system that can also scan maize plant structure for phenotyping. However, the technology was limited to a single plant, and the operation also limited the pace of the mobile robot. Using the Hough transform and a LiDAR sensor, a real-time guidance system was created [35]. The Hough transformation found a straight line for steering the vehicle by extracting plant rows. Curved row portions and other items in the way presented difficulties. A tractor was navigated through a citrus grove alleyway using machine vision and a LiDAR system [36], with the latter providing greater performance in straight and curved paths at speeds up to 3.1 km/h. The 360-degree LiDAR employed in the simulation presented in the paper has a maximum range of 8 m and a frequency of 7 Hz. The scan resolution is 1 measurement per 2 degrees.

The use of LiDAR for environment perception is prevalent in autonomous mobile robots and unmanned vehicles designed for use in urban environments. However, the atmosphere of a farm differs significantly from that of an indoor or urban setting. In an open agricultural setting, global navigation satellite system (GNSS) may offer accurate absolute positioning, however uneven farming grounds, less variant landmarks can create positioning error and distort LiDAR point cloud data [37]. The level of precision VFH algorithm requires is less, it looks at the overall structure of objects than in details. Li et al. [38] has

discussed that LIDAR with support of other positioning sensors at outdoor farm field environment perform better than at indoor based operations with over 80% success rate.

5. Methodology

The simulation is carried out in the MATLAB environment. During execution, the real-time values of observations were logged and saved in a CSV (Comma separated values) data file. The loop iterations were sampled typically every 120 milliseconds. The navigation platform toolbox is used to implement the PPA and VFH algorithm functions. For the LiDAR sensor application, the mobile robotic simulation toolbox is used. PPA is used in the simulation to achieve autonomous lateral navigation. The PPA the waypoint seeking system was guided by a steer guidance VFH algorithm against collision with obstacles. As shown in Fig. 3, different waypoints (P_1, P_2, P_3, P_4, P_5, and P_6) are constructed. With a change in size of coordinate data, these waypoints can be converted to GPS tagged points for real-world applications. The vehicle's robot localization is expected to be efficient, ignoring wheel slippage and drift. Odometry sensors, GPS, and motion sensors could be used in real-world models. The navigation route will cover points P_1 through P_6 in order. At the U bend of the row of plants shown in Fig. 2(b), the waypoints coordinates are formed as tip points alternately. The robot will navigate the field while avoiding various items; huge unavoidable obstructions will create a strong repulsive force field surrounding the vehicle, which will cause the robot to become immobile. The flowchart in Fig. 3 depicts the overall operation. The experiment is conducted on a vegetable field measuring 50 x 50 m^2. The robot experiment is carried out at various speeds. For each trial, the robot's speed was changed from 0.5 to 2.75 km/hr with a fixed speed. This speed range is ideal for slow operating irrigation robots that operate slowly. The robot will proceed in a zigzag cycle path to cover all rows of plants. The differential wheel robot has a 0.40 m wheelbase and a 10 cm wheel radius. After multiple trials and observations, the VFH parameters of histogram threshold value and number of angular sectors were calibrated and locked at an optimal value of 20. Even though the LiDAR sensor is two-dimensional, a synthetic two-dimensional imaging approach for navigation can be constructed from popular three-dimensional data [39]. This method also minimises the data and complexity associated with cloud point mapping.

Using image conversion from colour to black-and-white, a field image (Fig. 2(a)) is converted to a grid occupancy map (Fig. 2(b)). The occupancy map is a binary map with black parts representing obstructions and white parts representing open moveable space. Different obstacles, like as stones, solid items, or overgrown plants, may be present on the path as the robot advances along row gaps. The VFH algorithm assists in detecting and tactically avoiding static and moving impediments. The algorithm is based on the repellent forces produced by nearby obstructions. Every trial is recorded with scanned LiDAR sensor readings and pre-set PPA parameter values. The total distance D_c traversed by the robot is used to calculate the robot's deviation while travelling. More oscillations with a larger average deviation are indicated by a large distance D_c is distance travelled by the robot value. PPA characteristics that is desired linear velocity (D_{LV}), maximum angular velocity (AV_{max}), and minimum radius for turn (R_{min}) are tested in various ways. Sensor readings from location and object proximity are taken to determine optimal performance. The robot's total distance travelled in relation to time is an essential performance indicator.

The robot was expected to follow straight trajectories along the narrow gap. Marked trailed behind by the mobile robot help to visualize the deviation. The robotics expected to drive sharp close at U turns sections to prevent overshoot.

6. Results and observations

On various PPA settings, several sets of readings are taken. The desired linear velocity (DLV), Angular velocity maximum (AV_{max}), Lookahead distance (LD), and Minimum Radius are all varied in a total of 34 trials (R_{min}). Real time proximity distances are used to measure closeness of obstacles around the vehicle: Obstacle distance average (OD_{avg}), obstacle distance minimum (OD_{min}), and obstacle distance maximum (OD_{max}). OD_{max} is the robot's maximum or farthest distance maintained by vehicle from obstacles while travelling along the path. The nearest distance for the same is OD_{min}. The average obstacle distance maintained is OD_{avg}. Figs. 3 and 4 as well as Tables 1 and 2 depict observations. In each simulation, N_L is the number of loops or iterations consumed for completion of a trial, itis an accurate indicator of the experiment's time consumption. It represents the time it takes the mobile robot to get from waypoint P_1 to P_6. The distance travelled by the robot as it moves across the field is called D_c, and a smaller value is expected as usual for movement without oscillations.

The desired linear velocity (D_{LV}) is the speed of the moving vehicle. Slower speed produces lesser inertia of motion and hence lesser oscillations, however the time taken for completion of path is high. Such movement is suitable in slow field operations like watering of plants, weed removing etc. Force fields created by the obstacle objects are sub-

Table 1. Performance data with lookahead distance.

AV_{max} (rad/s)	N_L	D_c(m)	$OD_{avg}(m)$	OD_{min}(m)	OD_{max}(m)
2	2076	259	1.16	0.81	1.80
4	2076	259	1.16	0.81	1.80
6	2076	259	1.16	0.81	1.80
8	2076	259	1.16	0.81	1.80
10	2076	259	1.16	0.81	1.80
11	2088	260	1.20	0.81	1.51
12	2076	259	1.53	0.31	3.06
0.01	2093	261	1.25	0.81	1.57
0.06	2089	260	1.20	0.81	1.49
0.08	2085	260	1.20	0.81	1.51
0.001	2086	260	1.15	0.81	1.47

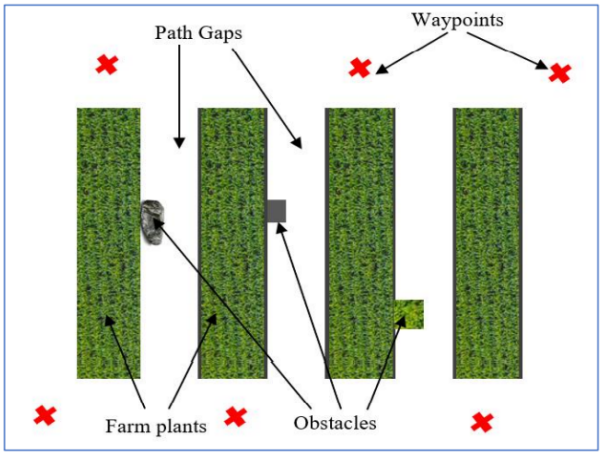

(a)

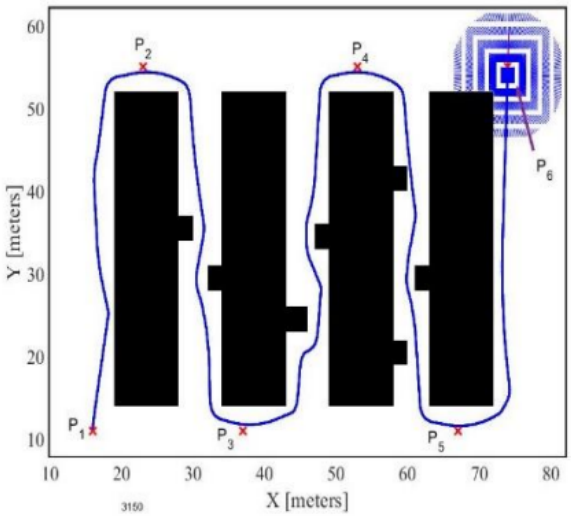

(b)

Fig. 2. (a) Real field image scenario. (b) field image with grid occupancy map.

tle, and the steering against obstacles are done smoothly, a more stable non deviated travel. The least obstacle distance

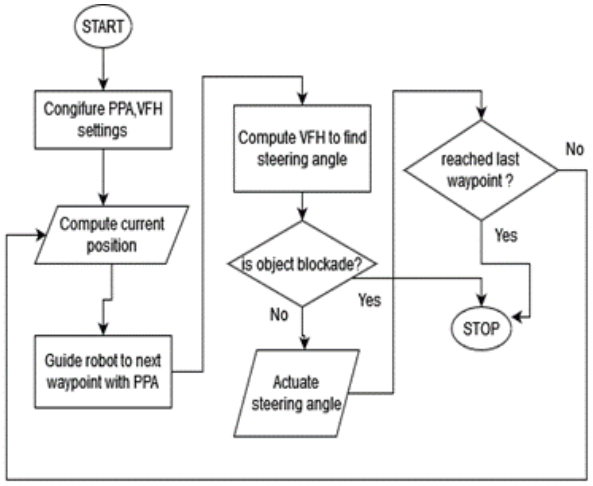

Fig. 3. Flowchart of overall operation.

OD_{avg} = 0.98 m when the D_{LV}=0.5 Km/Hr. The maximum value of OD_{avg} =1.40 m when D_{LV} =1.5 Km/Hr. Minimum value of N_L= 973 when D_{LV}=2.75 Km/Hr. Maximum value of N_L=4988 when D_{LV}=0.5 Km/Hr. Least distance D_C = 249 m when D_{LV} = 0.5 Km/Hr and maximum D_C =267 m when D_{LV} = 2.5 Km/Hr.

Maximum angular velocity (AV_{max})is highest limited value of angular velocity for the vehicle. It has a threshold value up to which performance is not much altered, but restricted beyond the limit. Mentioned observations are given in Table 1. The least value of OD_{avg} =1.16 m when AV_{max}= 2, the highest OD_{avg} =1.53 m when AV_{max} =12. Minimum value of N_L = 2076 at AV_{max}=2 rad/sec, maximum value of N_L=2093 at AV_{max} =0.01 rad/sec.

Lookahead distance (L_D) is an important factor effecting the lateral behavior of the vehicle. L_D is kept as constant value set before executing experiment. It is varied and tested at speed D_{LV} = 1.5 Km/Hr, an average speed chosen for the mobile robot. Lower value of L_D produces more oscillations but distance against obstacles and plants are

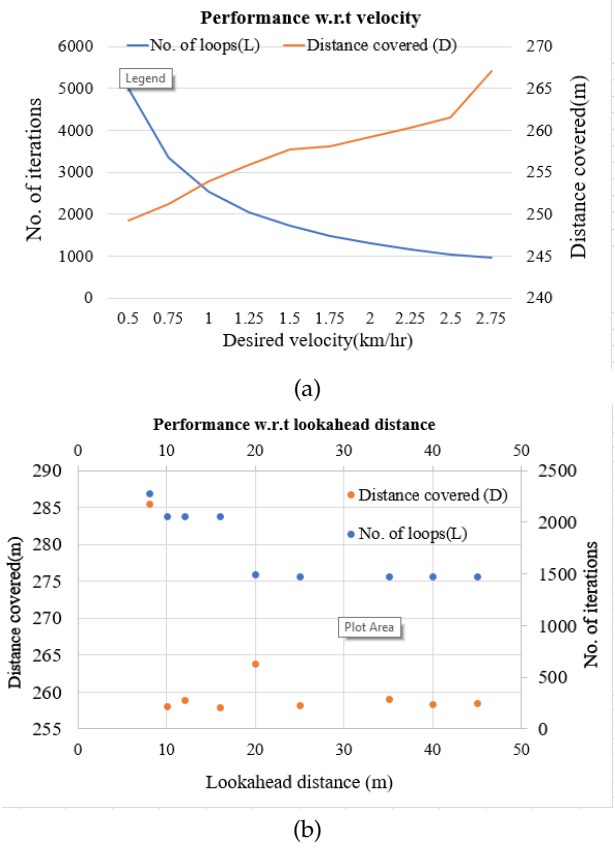

Fig. 4. (a) Performance plot under varying velocity of robot. (b) Performance plot under varying lookahead distance.

minimum. High oscillations consume more iteration and time. Observations are presented in Fig. 4. Minimum value of OD_{avg} =1.16 m occurred when L_D =12 m. OD_{avg} =1.39 m (highest) when L_D =45 m. Maximum number of loops N_L = 2286 when L_D =8 m, the minimum value of N_L=1510 when L_D =20 m. Maximum value of D_C = 285m when L_D = 8 m, minimum value D_C = 258 when L_D = 40 m. An optimum value of L_D = 20-25 m is chosen, where N_L=1478 is minimum and OD_{avg}=1.37 m.

Minimum radius R_{min} is another threshold value for turning radius scale. Its value had no impactful effect on the mobile robot performance. Insignificant changes are observed under distance of 3 meters (seen on Table 2) after which if increased the robot movement is disturbed due to large turn near row-end U sections.

6.1. Specific observations

The nearest obstacle distance OD_{avg} is most significantly influenced by desired linear velocity D_{LV} and lookahead distance L_D. It is to observe oscillations with respect to the different values of D_{LV}. A high value of 2 m is observed at linear velocity of 1.5 Km/Hr which again drops to 1.5 m at the velocity of 2.25 Km/Hr, again rising to higher value of 2.11 m at 2.75 Km/Hr. OD_{avg} increases with respect to value of L_D. OD_{avg} (=1.39) is highest at L_D =45 m and the lowest OD_{avg} (=1.17) at L_D =10 m. The shortest path taken by the robot is observed as 249 m low value with D_{LV}=0.5 m/s.

The fastest coverage of field is conducted within N_L=973 loops at D_{LV}= 2.75 Km/Hr. The slowest coverage is done in N_L= 4988 loops achieved at a low desired linear velocity of 0.5 Km/Hr (Fig. 4(a)). The vehicle gives an optimum speed D_{LV}=1.25km/hr with 2049 number of iteration loops. It can be seen in graph shown at Fig. 3, where the crossover points of two identifiers N_L and D_C. The N_L and D_C are intersecting for best performance results. Optimum lookahead distance is L_D =20 from where the number of loops is low with acceptable stability in its trajectory as seen in Fig. 4(b).

7. Conclusions

The experiment conducted the basic performance assessment of our LiDAR-based navigation system based on the needs of a simplified navigation system for an autonomous irrigation robot. The following characteristics have been summarised based on the above research and its experimental analysis:

(1) The VFH-based steering controller was used well in conjunction with PPA to avoid obstructions along the plantation gap. Keeping small number of waypoints reduces the mobile vehicle's setup time and oscillations.

(2) Choosing an appropriate lookahead distance and velocity are important parameters which are influenced by the robot's design, path size, manoeuvrability, and field type.

(3) Autonomous navigation was accomplished effectively by traversing all plant rows in a zigzag pattern. Multiple tests were conducted to evaluate the performance of the system. The least travel oscillations were seen at a speed of 0.5 km/h, while the highest speed covered was 2.75 km/h.

(4) The 2D grid occupancy mapping provides a straightforward method for overcoming autonomous navigation with less complex sensor data analysis. The procedure may be carried out on 16/32bit computer with minimum power usage. The range and performance of electric vehicles are largely dictated by their energy usage. The method designed by us can be useful for

Table 2. Performance data with lookahead distance.

R_{min}(m)	N_L	D_c(m)	OD_{avg}(m)	OD_{min}(m)	OD_{max}(m)
2	1478	258	1.33	0.94	1.67
4	1477	258	1.38	0.94	1.93
5	1494	261	1.35	0.97	1.85
3	1478	258	1.33	0.94	1.67

agricultural specific electric cars because of its low computational demand. It can increase the mileage and energy contribution of other field operations, such as pump machines and robotic arms.

The experiment has been conducted on barriers that are straight and rectangular, but it should function better in the actual world. Plants have rough surfaces on their leaves, stems, and branches, which improve readings of laser reflecting sensors. Planer surfacedeflect light signals at higher angle of incidence. Ignorable objects, such as little branches or leaves, might cause sensors to respond with an overly acute proportion causing the robot to stop. This issue can be resolved by using more effective planting procedures with well-maintained inter-row spaces for mobile robot. Remote monitoring and control override by human operator can be used to assist the robot in overcoming hurdles. The algorithm designed should certainly work for Level 2-3 autonomy of mobile robots which are more achievable than fully autonomous robots [40], the operator needs to occasionally control the robots. There are scopes to improve the sensory readings and analyze the data to observe different shapes and types of obstacles. Small U-shaped obstacles can trap the robot, algorithms can be developed to detect and divert from such objects at early. Discussed algorithm can also be studied and improved to different robot configuration of 4-wheel drive systems like Bonirob and Harvey [41].

Acknowledgment

The authors would like to acknowledge All India Council for Technical Education for financial assistance through Research Promotion Scheme (File No.8-2IFDC/RPS (NER)/POLICY-1/2020-21).

References

[1] V. B. Hans, (2016) *"Water management in agriculture: Issues and strategies in India"* **SSRN Electron**:

[2] X. Kan, T. C. Thayer, S. Carpin, and K. Karydis, (2021) *"Task Planning on Stochastic Aisle Graphs for Precision Agriculture"* **IEEE Robotics and Automation Letters** ***6***(2): 3287–3294. DOI: 10.1109/LRA.2021.3062337.

[3] *India's Rural Farmers Struggle to Read and Write. Here's How 'AgriApps' Might Change That. - GOOD*. https://www.good.is/articles/agricultural-apps-bridge-literacy-gaps-in-india. accessed: Jul. 17, 2022.

[4] *We still can't agree how to regulate self-driving cars - The Verge*. https://www.theverge.com/2020/2/11/21133389/house-energy-commerce-self-driving-car-hearing-bill-2020. accessed: Jul. 23, 2022.

[5] *Autonomous vehicles: How 7 countries are handling the regulatory landscape | TechRepublic*. https://www.techrepublic.com/article/autonomous-vehicles-how-7-countries-are-handling-the-regulatory-landscape/. accessed: Jul. 23, 2022.

[6] F. Zhang, W. Zhang, X. Luo, Z. Zhang, Y. Lu, and B. Wang, (2022) *"Developing an IoT-Enabled Cloud Management Platform for Agricultural Machinery Equipped with Automatic Navigation Systems"* **Agriculture (Switzerland)** ***12***(2): DOI: 10.3390/agriculture12020310.

[7] T. S. Hong, D. Nakhaeinia, and B. Karasfi, (2012) *"Application of fuzzy logic in mobile robot navigation"* **Fuzzy Logic-Controls, Concepts, Theories and Applications**: 21–36.

[8] I. Susnea, A. Filipescu, G. Vasiliu, G. Coman, and A. Radaschin. "The bubble rebound obstacle avoidance algorithm for mobile robots". In: Cited by: 12. 2010, 540–545. DOI: 10.1109/ICCA.2010.5524302.

[9] T. S. Abhishek, D. Schilberg, and A. S. A. Doss. "Obstacle avoidance algorithms: A review". In: *IOP Conference Series: Materials Science and Engineering*. ***1012***. 1. IOP Publishing. 2021, 012052.

[10] A. Ohya, A. Kosaka, and A. Kak, (1998) *"Vision-based navigation by a mobile robot with obstacle avoidance using single-camera vision and ultrasonic sensing"* **IEEE Transactions on Robotics and Automation** ***14***(6): 969–978. DOI: 10.1109/70.736780.

[11] S. A. Hiremath, G. W. van der Heijden, F. K. van Evert, A. Stein, and C. J. Ter Braak, (2014) *"Laser range finder model for autonomous navigation of a robot in a maize field using a particle filter"* **Computers and**

Electronics in Agriculture *100*: 41–50. DOI: 10.1016/j.compag.2013.10.005.

[12] J.-K. Yoo and J.-H. Kim, (2015) *"Gaze Control-Based Navigation Architecture with a Situation-Specific Preference Approach for Humanoid Robots"* **IEEE/ASME Transactions on Mechatronics *20***(5): 2425–2436. DOI: 10.1109/TMECH.2014.2382633.

[13] S. Sukkarieh, E. M. Nebot, and H. F. Durrant-Whyte, (1999) *"A high integrity IMU/GPS navigation loop for autonomous land vehicle applications"* **IEEE Transactions on Robotics and Automation *15***(3): 572–578. DOI: 10.1109/70.768189.

[14] M. Gilmartin, (2005) *"INTRODUCTION TO AUTONOMOUS MOBILE ROBOTS, by Roland Siegwart and Illah R. Nourbakhsh, MIT Press, 2004, xiii+ 321 pp., ISBN 0-262-19502-X.(Hardback,£ 27.95)"* **Robotica *23***(2): 271–272.

[15] X. Gao, J. Li, L. Fan, Q. Zhou, K. Yin, J. Wang, C. Song, L. Huang, and Z. Wang, (2018) *"Review of wheeled mobile robots' navigation problems and application prospects in agriculture"* **IEEE Access *6***: 49248–49268. DOI: 10.1109/ACCESS.2018.2868848.

[16] K. Zhu and T. Zhang, (2021) *"Deep reinforcement learning based mobile robot navigation: A review"* **Tsinghua Science and Technology *26***(5): 674–691. DOI: 10.26599/TST.2021.9010012.

[17] *"Bosch's Giant Robot Can Punch Weeds to Death - IEEE Spectrum*. https://spectrum.ieee.org/bosch-deepfield-robotics-weed-control. accessed: Jan. 26, 2022.

[18] A. Roshanianfard, N. Noguchi, H. Okamoto, and K. Ishii, (2020) *"A review of autonomous agricultural vehicles (The experience of Hokkaido University)"* **Journal of Terramechanics *91***: 155–183. DOI: 10.1016/j.jterra.2020.06.006.

[19] W. Zhao, X. Wang, B. Qi, and T. Runge, (2020) *"Ground-level Mapping and Navigating for Agriculture based on IoT and Computer Vision"* **IEEE Access**: DOI: 10.1109/ACCESS.2020.3043662.

[20] W. Yuan, Z. Li, and C.-Y. Su, (2021) *"Multisensor-Based Navigation and Control of a Mobile Service Robot"* **IEEE Transactions on Systems, Man, and Cybernetics: Systems *51***(4): 2624–2634. DOI: 10.1109/TSMC.2019.2916932.

[21] F. Rovira-Mas, V. Saiz-Rubio, and A. Cuenca-Cuenca, (2021) *"Augmented Perception for Agricultural Robots Navigation"* **IEEE Sensors Journal *21***(10): 11712–11727. DOI: 10.1109/JSEN.2020.3016081.

[22] N. Gupta, M. Khosravy, S. Gupta, N. Dey, and R. G. Crespo, (2022) *"Lightweight Artificial Intelligence Technology for Health Diagnosis of Agriculture Vehicles: Parallel Evolving Artificial Neural Networks by Genetic Algorithm"* **International Journal of Parallel Programming *50***(1): DOI: 10.1007/s10766-020-00671-1.

[23] E. Horvath, C. Hajdu, and P. Koros. "Novel Pure-Pursuit Trajectory Following Approaches and their Practical Applications". In: Cited by: 4. 2019, 597–602. DOI: 10.1109/CogInfoCom47531.2019.9089927.

[24] X. Wang, G. Tan, Y. Dai, F. Lu, and J. Zhao, (2020) *"An Optimal Guidance Strategy for Moving-Target Interception by a Multirotor Unmanned Aerial Vehicle Swarm"* **IEEE Access *8***: 121650–121664. DOI: 10.1109/ACCESS.2020.3006479.

[25] J. Lopez, P. Sanchez-Vilarino, R. Sanz, and E. Paz, (2021) *"Efficient Local Navigation Approach for Autonomous Driving Vehicles"* **IEEE Access *9***: 79776–79792. DOI: 10.1109/ACCESS.2021.3084807.

[26] T. Bouwmans, (2014) *"Traditional and recent approaches in background modeling for foreground detection: An overview"* **Computer Science Review *11-12***: 31–66. DOI: 10.1016/j.cosrev.2014.04.001.

[27] J. S. Kulchandani and K. J. Dangarwala. "Moving object detection: Review of recent research trends". In: Cited by: 87. 2015. DOI: 10.1109/PERVASIVE.2015.7087138.

[28] G. Qi, H. Wang, M. Haner, C. Weng, S. Chen, and Z. Zhu, (2019) *"Convolutional neural network based detection and judgement of environmental obstacle in vehicle operation"* **CAAI Transactions on Intelligence Technology *4***(2): 80–91. DOI: 10.1049/trit.2018.1045.

[29] J. Borenstein and Y. Koren, (1989) *"Real-Time Obstacle Avoidance for Fast Mobile Robots"* **IEEE Transactions on Systems, Man and Cybernetics *19***(5): 1179–1187. DOI: 10.1109/21.44033.

[30] J. Borenstein, Y. Koren, et al., (1991) *"The vector field histogram-fast obstacle avoidance for mobile robots"* **IEEE transactions on robotics and automation *7***(3): 278–288.

[31] W. Zhang, H. Cheng, L. Hao, X. Li, M. Liu, and X. Gao, (2021) *"An obstacle avoidance algorithm for robot manipulators based on decision-making force"* **Robotics and Computer-Integrated Manufacturing *71***: DOI: 10.1016/j.rcim.2020.102114.

[32] Z. Chong, B. Qin, T. Bandyopadhyay, M. Ang, E. Frazzoli, and D. Rus. "Synthetic 2D LIDAR for precise vehicle localization in 3D urban environment". In: Cited by: 90. 2013, 1554–1559. DOI: 10.1109/ICRA.2013.6630777.

[33] Y. Li and J. Ibanez-Guzman, (2020) *"Lidar for Autonomous Driving: The Principles, Challenges, and Trends for Automotive Lidar and Perception Systems"* **IEEE Signal Processing Magazine** ***37***(4): 50–61. DOI: 10.1109/MSP.2020.2973615.

[34] U. Weiss and P. Biber, (2011) *"Plant detection and mapping for agricultural robots using a 3D LIDAR sensor"* **Robotics and Autonomous Systems** ***59***(5): 265–273. DOI: 10.1016/j.robot.2011.02.011.

[35] O. C. Barawid Jr., A. Mizushima, K. Ishii, and N. Noguchi, (2007) *"Development of an Autonomous Navigation System using a Two-dimensional Laser Scanner in an Orchard Application"* **Biosystems Engineering** ***96***(2): 139–149. DOI: 10.1016/j.biosystemseng.2006.10.012.

[36] V. Subramanian, T. F. Burks, and A. Arroyo, (2006) *"Development of machine vision and laser radar based autonomous vehicle guidance systems for citrus grove navigation"* **Computers and Electronics in Agriculture** ***53***(2): 130–143. DOI: 10.1016/j.compag.2006.06.001.

[37] Y. Ji, S. Li, C. Peng, H. Xu, R. Cao, and M. Zhang, (2021) *"Obstacle detection and recognition in farmland based on fusion point cloud data"* **Computers and Electronics in Agriculture** ***189***: DOI: 10.1016/j.compag.2021.106409.

[38] N. Li, L. Guan, Y. Gao, S. Du, M. Wu, X. Guang, and X. Cong, (2020) *"Indoor and outdoor low-cost seamless integrated navigation system based on the integration of INS/GNSS/LIDAR system"* **Remote Sensing** ***12***(19): 1–21. DOI: 10.3390/rs12193271.

[39] M. Samuel, M. Hussein, and M. B. Mohamad, (2016) *"A review of some pure-pursuit based path tracking techniques for control of autonomous vehicle"* **International Journal of Computer Applications** ***135***(1): 35–38.

[40] J. Lowenberg-DeBoer, K. Behrendt, M.-H. Ehlers, C. Dillon, A. Gabriel, I. Y. Huang, I. Kumwenda, T. Mark, A. Meyer-Aurich, G. Milics, K. O. Olagunju, S. M. Pedersen, J. Shockley, and D. Rose, (2022) *"Lessons to be learned in adoption of autonomous equipment for field crops"* **Applied Economic Perspectives and Policy** ***44***(2): 848–864. DOI: 10.1002/aepp.13177.

[41] O. Bawden, D. Ball, J. Kulk, T. Perez, and R. Russell. "A lightweight, modular robotic vehicle for the sustainable intensification of agriculture". In: ***02-04-December-2014***. Cited by: 24. 2014.